Environmental Effects on Poly-*p*-phenylenebenzobisoxazole Fibers. I. Mechanisms of Degradation

Peter J. Walsh,[1] Xianbo Hu,[1] Philip Cunniff,[2] Alan J. Lesser[1]

[1]*Polymer Science and Engineering Department, University of Massachusetts, Amherst, Massachusetts 01003*
[2]*US Army Soldier Systems Center, Natick, Massachusetts 01760*

Received 9 March 2006; accepted 21 April 2006
DOI 10.1002/app.24788
Published online in Wiley InterScience (www.interscience.wiley.com).

ABSTRACT: This is the first of a two-part series investigating the degradation mechanisms of PBO fiber and approaches to alleviating degradation and improving fiber properties. Poly-*p*-phenylenebenzobisoxazole (PBO) fiber is a high strength and modulus fiber with remarkable thermal stability. Recent in-service failures of this fiber have revealed that the fiber degrades rapidly in relatively mild environmental conditions of moisture and heat. In this work the mechanisms of degradation due to moisture, the presence of acid, and the effect of radiation from the UV–vis spectrum are investigated. It is found that exposure to moisture results in the loosening of the fiber morphology leading to an increase in the number and size of defects. The presence of aqueous acid causes both loosening of the fiber structure and hydrolysis of the oxazole ring structure. The effect of UV–vis radiation is primarily hydrolysis of the material near the fiber surface with attendant formation of amide linkages. © 2006 Wiley Periodicals, Inc. J Appl Polym Sci 102: 3517–3525, 2006

Key words: poly(benzoxazole) fiber; PBO; physical degradation; chemical degradation; SAXD; WAXD; ATR-FTIR

INTRODUCTION

Poly-*p*-phenylenebenzobisoxazole (PBO) is one of a family of isotropic liquid crystalline polymers that orient easily into extended chain configurations producing fibers with excellent strength and modulus. PBO polymer was originally developed by the U.S. Air Force to replace metals in space and aviation applications for its excellent thermal stability and chemical resistance.[1] PBO fibers typically have exceptionally high tensile strength (5.8 GPa), stiffness (180–270 GPa), and relatively low density (1.54 g/cm^3).[2–4] To date, they are the strongest commercially available organic polymeric fibers. Consequently, they are ideal candidates for many military applications. Research and development of this material is being actively pursued for applications in high-performance fiber composites, protective garments, and personnel ballistic armors.

Recently (late 2001), Toyobo published some disconcerting results regarding the susceptibility of PBO fibers to degradation when exposed to relatively mild conditions.[5] In particular, the strength of PBO fibers decreases even at a temperature less than 100°C in high humidity. After 100 days at 80% relative humidity, and 80°C more than 40% of the strength is lost and the trend in the data suggest that additional losses can be expected with continued exposure. Subsequent data from Toyobo show that PBO fibers are also susceptible to degradation when exposed to sunlight. Both AS and HM fibers lose more than 50% of their strength after only 3 months exposure at Ohtsu, Japan. Toyobo has shown similar results with 100 days' exposure in a Xenon arc weatherometer. Subsequent to these reports, numerous news reports reiterating these concerns in PBO products have been reported.[6]

POTENTIAL DEGRADATION MECHANISMS

The reported propensity of PBO fibers to degrade when exposed to sunlight and/or high humidity is somewhat surprising given the apparent high thermal and chemical stability of this class of polymers. To date, no mechanism has been confirmed to explain the degradation in mechanical properties of PBO fibers when exposed to relatively mild conditions. However, potential mechanisms can be proposed after considering how commercial fibers are made.

Commercial PBO fibers are spun using a dry-jet wet spinning process. In this process, PBO polymer solution containing 10–20% of PBO in polyphosphoric acid (PPA) is extruded through a spinneret into a coagulation bath (water). This is followed by washing, drying and, in the case of HM fiber, heat treatment. The structure formed during the coagulation stage of the above dry-jet-wet-spinning process of PBO fiber is an interconnected network of oriented microfibrils, the

Correspondence to: A. J. Lesser (ajl@mail.pse.umass.edu).
Contract grant sponsors: U.S. Army Research Office and the International Association of Fire Fighters.

width of which is 8–10 nm. These were confirmed by Thomas.[7–9] These microfibrils are the fundamental structural elements of the final fibers. PBO fibers after the solvation, however, contain a great amount of the nonsolvent in 25% by weight or more, and they will exhibit a volume change on drying. During drying, the network is collapsed to yield the ''as-spun'' fiber.[10] Consequently, there are inevitably defects present in the fibers, which have been verified with small-angle X-ray scattering and transmission electron microscopy.[11] The voids are elongated in the direction of the fiber axis.

PHYSICAL MECHANISMS

There are two primary reasons for us to focus on the physical aspects of fiber degradation. First, the fiber tenacity is related to the concentration of defects, which act as fracture initiation sites. The process used to manufacture PBO fiber results in a necessary introduction of microvoids and these defects act as fracture initiation sites. Second, because there are only relatively weak van der Waals and electrostatic forces acting between chains, slippage of adjacent crystalline domains and fibrils is possible. Within this context, the size and concentration of the microvoids, or even the interconnectivity between fibrils and microvoids may be changed under certain conditions and the resulting morphology will definitely influence the mechanical properties of PBO fibers.

On the basis of the unique molecular, crystalline, and supermolecular structures of PBO fibers, we hypothesize that any environmental factor, which can loosen the structure of PBO fibers, such as introducing defect on fiber surface or inside the fiber, weakening the interfacial adhesion between fibrils and crystals, will decrease the mechanical properties of PBO fiber. On the other hand, any treatment that can densify the structure of PBO fiber such as increasing the orientation and size of crystals and fibrils, increasing the interfacial interactions between fibrils, may increase the mechanical properties of PBO fibers. This topic will be explored further in Part II of this paper; Part I will focus on determining the physical and chemical mechanisms of PBO fiber degradation.

CHEMICAL MECHANISMS

It was observed some time ago that the coagulation of PBO in methylsulfonic acid (MSA) solution with water was accompanied by a decrease of polymer intrinsic viscosity (IV). Berry[12] and Metzger[13] proposed that the IV decrease was not due to chain scission, but was a result of interchain association, with the chains in parallel array in the aggregates. Recent study indicates that PBO in PPA or MSA with residual water followed by coagulation in water underwent bond cleavage to generate carboxylic acid and *o*-aminophenol functional groups.[14] Bourbigot proposed the chain cleavage during pyrolysis of PBO and showed that oxygen plays a great role in the thermooxidative degradation, which is an initiator of degradation.[15] In addition, the conjugated structure of the PBO mer and π-π stacking in PBO crystals may make the fiber intrinsically photosensitive.[16]

Although these severe conditions are unlikely to be encountered in normal applications of PBO fibers, we must consider that PBO fiber is spun from a solution of PPA, and it is reasonable to expect that trace phosphoric residuals in the fibers combined with wet or humid environments, sunlight and oxygen may promote hydrolytic degradation.

In this work, we will look for evidence of physical and chemical degradation pathways for fibers exposed to aqueous environments, acidic environments and radiation in the ultraviolet–visible light range. Subsequent to exposure fibers will be characterized using a broad range of mechanical and physical tests including tensile testing, scanning electron microscopy (SEM), small-angle X-ray diffraction (SAXD), wide-angle X-ray diffraction (WAXD), and attenuated total reflectance infrared spectroscopy (ATR-FTIR).

EXPERIMENTAL

Materials

PBO fiber used in these experiments is Zylon AS, which was supplied by US Army Soldier Systems Center at Natick, MA. The related properties of the fiber can be found in Ref. 2.

Procedures

Liquid and vapor water exposure

Tows of PBO AS fibers were placed in liquid deionized water in a dessicator and held at 50°C in a darkened oven. PBO tows were exposed to water vapor by placing them above deionized water held within a second dessicator and held at 50°C in the same oven. The relative humidity within the dessicator was measured at 90% under these conditions. Fibers were periodically removed from both environments and dried at room temperature prior to any characterization experiments.

Phosphoric acid exposure

Phosphoric acid solutions of 0.5*M*, 1*M*, and 1.8*M* concentration were prepared from deionized water and 85% *o*-phosphoric acid obtained from Fisher Chemical and used as received. Tows of PBO AS fibers were placed in the acid solution within a closed darkened container at 20°C. Tows of fiber were periodically

removed and dried for 24 h under vacuum prior to tensile testing or other characterization.

UV–visible light exposure

Controlled exposure to UV–visible light was accomplished using a Suntest CPS+ weatherometer. The radiation source is a xenon lamp with a broad spectrum filter that closely simulates the distribution of wavelengths and intensity found in natural sunlight. The fibers were exposed to at 750 W/m^2 and held at a constant temperature of 50°C. Fibers used for tensile testing were single fibers fastened to cardboard backing with an epoxy adhesive and placed in the CPS+ Suntester sample tray, fibers used for SEM, SAXD, WAXD, and ATR-FTIR were tows each comprised of approximately 160 single fibers and placed in the sample tray in parallel arrays.

Tensile testing

Mechanical properties were measured using an Instron 5800 series tensile tester with a 50 N load cell. Tests were conducted on single fiber specimens using a crosshead velocity of 10 mm/min and a gauge length of 20 mm. The single fiber samples were glued at each end to a cardboard backing using Huntsman Araldite 2012 five-minute epoxy. Two holes in the cardboard backing were used to ensure a consistent gauge length. The center section of the backing was removed after the sample was fixed in the Instron grips. The grips were arranged with pin ends between the Instron foundation and the gripping surface so the direction of applied force and fiber axis were coincident. Each reported value of breaking strength, modulus, and elongation at break is the mean from a population of at least 15 single fiber tests.

Scanning electron microscopy

SEM images were collected using an JEOL 6320FXV high resolution field emission cold cathode scanning electron microscope with semi-in-lens detector configuration achieving resolution down to 2 nm. Mounted fiber samples were sputter coated with gold in an argon atmosphere.

ATR-FTIR

ATR-FTIR spectra were collected using a Horiba HR800 Lab-Ram microscope with resolution of 4 cm^{-1}. Fiber samples were prepared by laying a tow of fibers over a clean glass microscope slide. Three spectra were collected at different locations on the sample for each type of fiber to assure that the spectra are truly representative of the fiber surface condition.

SAXD, WAXD

SAXD measurements were performed on tows of fiber using a Molecular Metrology(®SAXD device. SAXD images were calibrated using a turkey tendon standard. WAXD measurements were performed using a Rigaku RU-H3R rotating anode X-ray diffractometer (operating at 1.2 kW, equipped with a multilayer focusing optic: point focus (100 μm)^2; Osmic Inc., type CMF23–46Cu8) and a home built evacuated Statton-type scattering camera. Scattering patterns were acquired with a 10 cm × 15 cm Fuji ST-VA image plates in conjunction with a Fuji BAS-2500 image plate scanner.

Elemental analysis

Carbon, hydrogen, and nitrogen analysis is performed by precisely weighing 2500–3500 μg of sample and combusting it at 1000°C in oxygen over a platinum catalyst, using a standardized Exeter Analytical 240XA Elemental Analyzer based on the modified Pregl-Dumas method. Phosphorus analysis is performed by a standard inductively coupled plasma emission spectroscopy (ICP) technique, after 20–30 mg of sample is precisely weighed and digested with a combination of sulfuric and nitric acids. A Leeman Labs, Direct Reading Echelle (DRE) ICP was utilized.

RESULTS AND DISCUSSION

Liquid and vapor phase water exposure results

Figure 1 shows the results of tensile testing for PBO AS fibers immersed in liquid–water at room temperature and conditioned in 90% relative humidity at 50°C respectively. Both treatments decrease tenacity and the strain at break while modulus remains essentially constant. Two key facts are evident: first, moisture alone

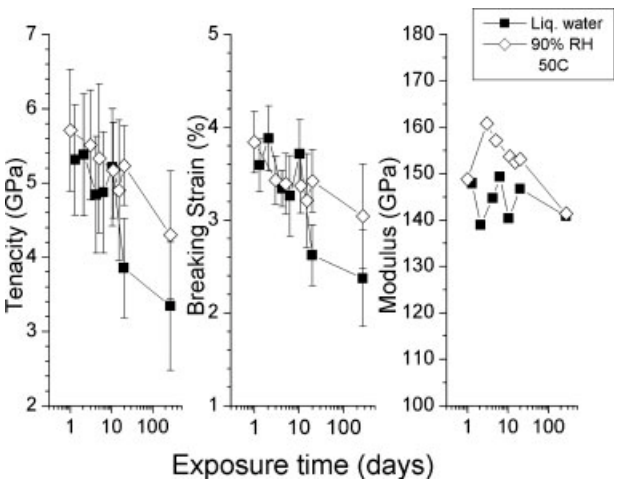

Figure 1 Tensile data for PBO fiber exposed to liquid water and 90% relative humidity at 50°C.

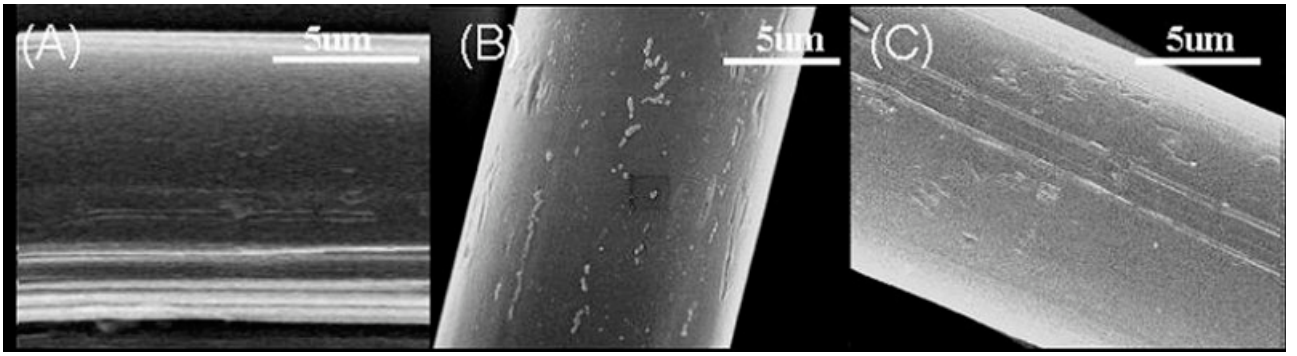

Figure 2 SEM micrographs: (A) PBO AS control, (B) PBO AS fiber exposed to liquid water, (C) PBO AS fiber exposed to 90% relative humidity.

does degrade the mechanical strength of the fibers, and fibers immersed in liquid–water degrade more quickly than those in humid environments.

The Figure 2 SEM micrographs compare the surfaces of (A) undegraded PBO fiber with (B) PBO AS fiber exposed to liquid–water for 270 days at 50°C and (C) PBO AS fiber exposed to 90% relative humidity at 50°C for 270 days. In both types of moisture-exposed fiber, the development of long defects parallel to the fiber axis is observed. One possibility is that these surface defects are a result of voids increasing in size with water exposure and breaking through the fiber surface.

To examine changes in the size and shape of voids within the fiber bundle SAXD patterns of a tow of parallel fibers were collected as a function of liquid–water exposure. Figure 3 shows the diffraction pattern and Guinier plot for liquid–water exposed PBO AS fiber. Previous work by Kitigawa, in which TEM images of axially sectioned fiber were compared with the correlation length from SAXD, has confirmed that the equatorial streak is due to scattering by needle-like voids oriented parallel to the fiber axis rather than the fibrillar elements.[17]

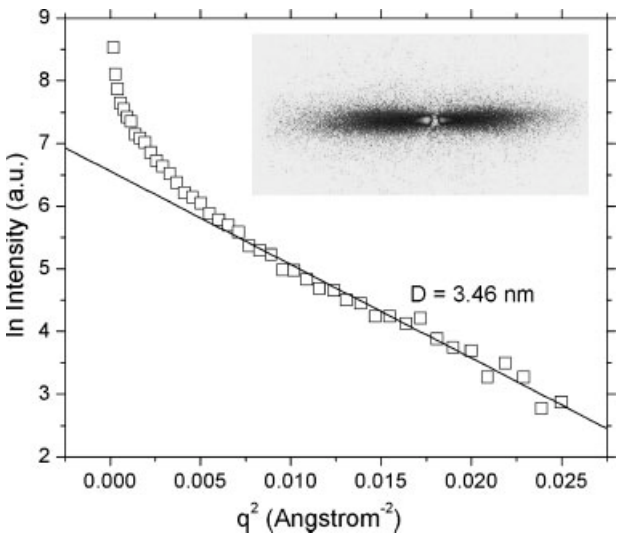

Figure 3 SAXD diffraction pattern and Guinier plot for PBO fiber exposed to liquid water.

Table I shows the correlation length (D) of the void cross section according to the wide angle region of a Guinier plot, and from the small angle regions, the radius of gyration of the void cross section (R_3), the mean-length across the void cross section parallel to the incident beam (l_2), and the void cross-sectional area (S_3) using the analysis of Shioya.[18]

D, R_3, l_2 all remain approximately constant while S_3 increases with exposure implying that the fiber has become swollen. If we approximate these voids as needlelike ellipsoids oriented parallel to the fiber axis and with major and minor cross-sectional axes randomly arranged through the fiber it is reasonable that R_3 does not change significantly as the fiber swells. This quantity is an indication of the radius of gyration of the void cross section. If the cross section is elliptical the radius of gyration will change as the root mean square of the major and minor axes. With the high aspect ratio of major and minor axes indicated by the comparison of S_3 and D, the change in the length of these axes is small and so will be the effect on R_3. The random orientation of the major and minor axes of the void cross section means that D and l_2 will remain approximately constant because the decrease in mean length of a void cross section oriented with major axis parallel to the incident beam will be offset by the increase in mean

TABLE I
Results of Guinier Plot and SAXD Analysis for Liquid–Water Exposed PBO Fiber

Sample (d)	D (Å)	R_3 (Å)	l_2 (Å)	S_3 (Å^2)
Control	34.6	31.1	42.4	12.03
20	34.6	30.3	38.0	13.89
150	33.4	30.3	37.7	16.06
270	32.9	31.6	31.6	17.86

[a] The increase in the average cross sectional area (S_3) of the voids suggests a loosening of the fibrillar bundle on exposure to water.

length of one with major axis perpendicular to the incident beam. The increase in S_3 implies that the void cross sections are becoming more circular with exposure. These observations taken in context with the SEM evidence of Figure 2 for increased void size are consistent with a permanent swelling of the fibrillar bundle by moisture.

This change in fiber structure is a very likely cause for the large drop in fiber strength and elongation at break. As the fiber swells voids may be growing along the fiber axis. Adjacent voids may be coalescing to form larger defects and new voids may be nucleating. The net effect is to increase the number of defects present in a given fiber. The increased size of the defects leads to a greater number becoming preferential sites for fracture initiation leading to a decrease in fiber strength and elongation at break.

As mentioned previously, it has been suggested that residual phosphoric acid within the fiber may play a role in the degradation process when water is present. ATR-FTIR was used to evaluate possible chemical changes in the PBO fiber with exposure to water. Figure 4 is a comparison of spectra for a PBO AS control fiber and various durations of liquid–water exposure. The IR spectra show no indication of any chemical changes near the fiber surface. WAXD data also indicate no changes on the length scale of the crystalline domains within the PBO fibrils (Fig. 5).

Taken together these SEM, SAXD, ATR-FTIR, and WAXD observations suggest that there is no large degree of chemical degradation occurring with exposure to water and that the mechanism of degradation appears to be primarily a physical one in which the fibrillar elements within the fiber are loosened. The resulting increase in size of the microvoid defects

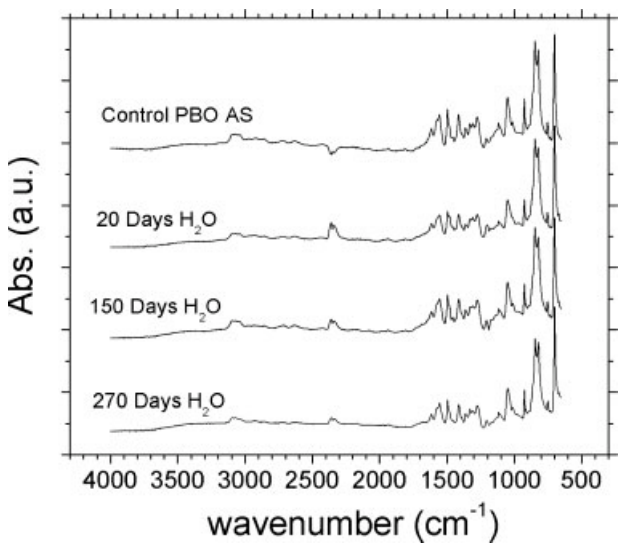

Figure 4 ATR-FTIR spectra for PBO fiber exposed to liquid water showing that there is no significant alteration of the chemical structure at or near the surface of the fibers. Spectra of fiber exposed to water vapor showed similar results.

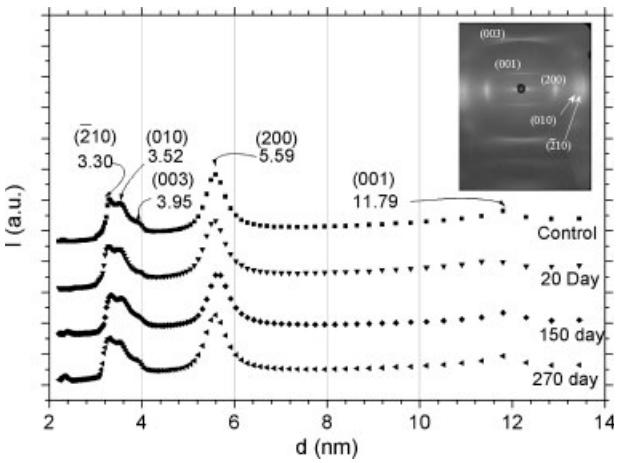

Figure 5 WAXD results for PBO AS fiber exposed to liquid water showing no effect on the crystalline structure of the fiber.

present in the fiber is the primary cause of the loss in strength. However, work assessing the effects of phosphoric acid on fiber morphology and strength suggests that even small concentrations of acid may accelerate the growth of defects and loss of strength.

Effects of residual phosphoric acid

Elemental analysis was initially done on the Zylon AS fiber to determine whether residual phosphoric acid resides in the fiber, and if so, establish a baseline quantity. Our results from these analyses indicate that an amount of residual phosphorus ranging between 0.3 and 0.4 wt % resides in the fiber. This result supports hypothesis of degradation involving phosophoric acid in that residual phosphorous, which may be in the form of phosphoric acid is certainly present in the fibers.

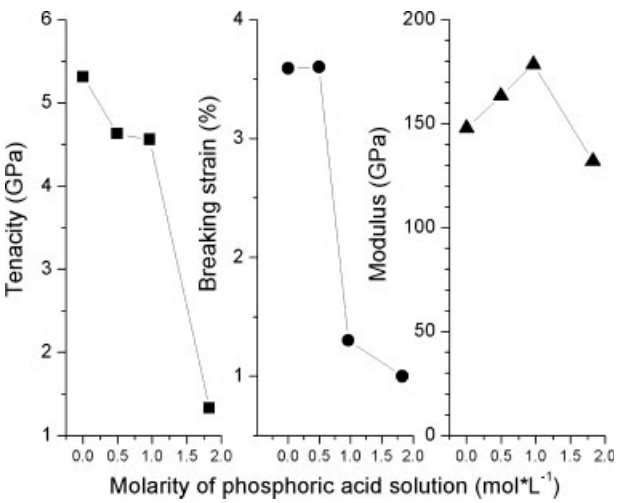

Figure 6 Tensile testing results for PBO fiber for 24 h exposure to increasing concentrations of aqueous phosphoric acid solution.

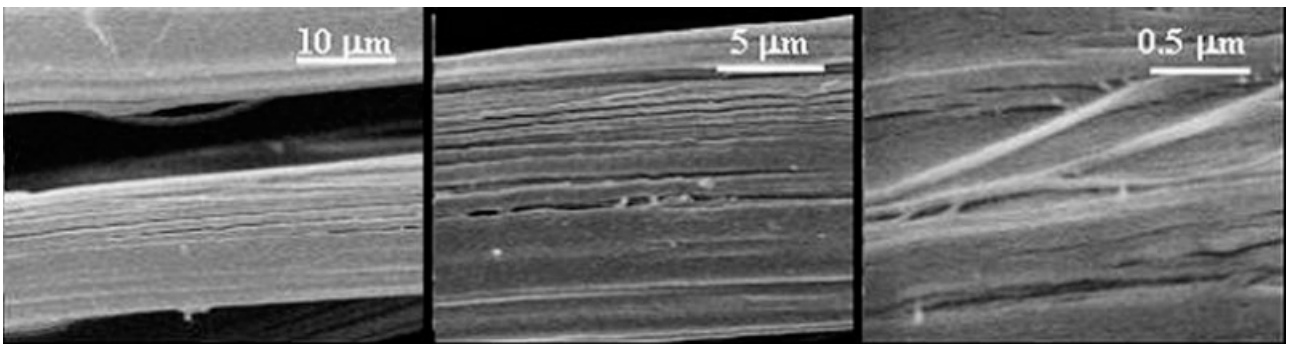

Figure 7 SEM results for PBO fiber exposed to 1.8*M* phosphoric acid.

To assess whether residual PA contributes the reported mechanical degradation, PBO fibers were conditioned in various PA/H_2O solutions for 24 h at room temperature, dried under vacuum for 24 h and characterized for residual phosphoric acid. Using this approach allowed for adjusting the residual phosphorus in a controlled way between 0.3 and 4.8 wt %.

Chemical exposure results

PBO AS fibers were exposed to 0.5*M*, 1*M*, and 1.8*M* phosphoric acid solution. Subsequent elemental analysis of these fibers indicated 0.3, 0.7, and 4.8 wt % of residual phosphorus for each concentration. Figure 6 shows the tenacity, breaking strain, and modulus of the exposed fibers. At stronger concentration, the reduction in strength is on the order of 75%. Based on our previous observations in which fiber strength was not significantly changed by 24 h exposure to liquid–water, it is reasonable to assume this drop in properties to be due to chemical degradation and not the physical mechanism proposed for water exposure. However, examination of the Figure 7 SEM results shows that there is certainly significant physical separation of fibrillar elements occurring.

The ATR-FTIR spectra shown in Figure 8 compare neat fiber with liquid–water exposed and phosphoric acid exposed fiber. The broad band of absorbance centered $\sim 3400\ cm^{-1}$ increases slightly for the phosphoric acid/PBO samples and a new peak at $\sim 3200\ cm^{-1}$ occurs. The first are assigned to an amide N—H and the second to a cyclic N—H. There is also a small increase in absorbance at 1600–1700 cm^{-1} indicating the presence of amide carbonyls or other C—O.

While these spectra do not illuminate the exact chemical mechanism of degradation it is clear that a chemical reaction is occurring and they suggest that hydrolysis of the oxazole ring is the most likely route. The physical separation of the fibrillar elements observed in the SEM indicates that the chemical reactions with strong acid will accelerate the increase in defect size and number. This is relevant to the earlier observations for liquid–water exposed fiber because it is possible that even very low concentrations of phos-

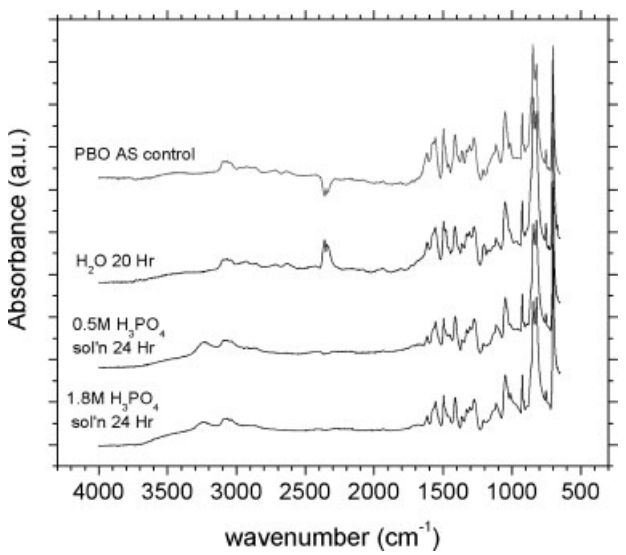

Figure 8 ATR-FTIR results for PBO Fiber exposed to increasing concentrations of phosphoric acid.

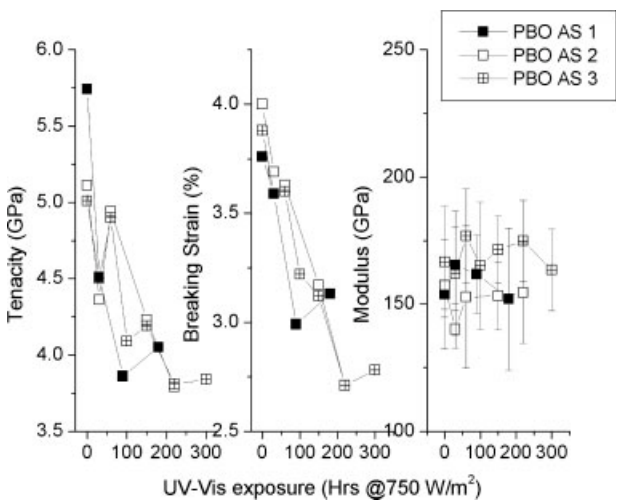

Figure 9 Tensile testing results for three series of PBO AS fiber exposed to UV–vis light at an intensity of 750 W/m^2. Error bars on modulus indicate one standard deviation about the mean value.

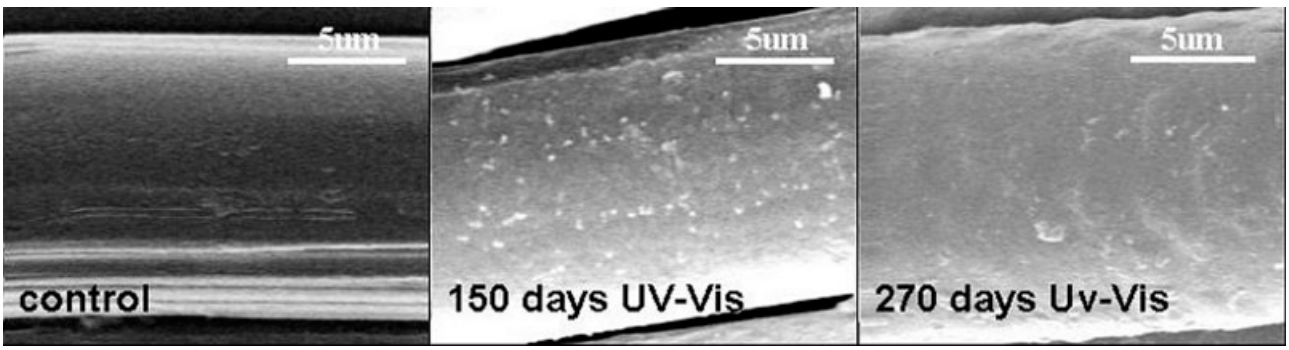

Figure 10 SEM results for UV–visible light exposed PBO AS fiber.

phoric acid will have a similar effect while not causing chemical change in enough of the fiber surface to show changes in the ATR-FTIR spectra.

UV–visible light exposure

Figure 9 shows the effects of exposure to UV–visible light for three series of tests on PBO AS fiber. Tenacity and breaking strain are both reduced by approximately 40% after 300 h of exposure with significant losses occurring after only the first 100 h interval. The data for modulus shows that it is highly variable for a given exposure time but within these limits can be considered to remain approximately constant with UV–vis exposure.

The SEM results of Figure 10 compare pristine PBO AS fiber with fibers exposed to UV–vis light at 750 W/m^2 for durations of 150 and 270 days. As compared to the control fiber, it can clearly be seen that the material on the UV–vis exposed fiber surface has lost orientation. It seems very likely that the chemical nature of the polymer backbone is altered. While the depth of degradation cannot be determined from these images small degrees of degradation at the fiber surface will result in large changes in the cross-sectional area available to bear load. In addition work by Kitigawa shows that PBO AS fiber has a core-shell structure in which the shell of approximately 1–2 μm depth has fewer voids and a higher degree of order than core region. Loss of a fairly small proportion of the fiber shell region may have a disproportionately large effect on fiber strength.

Possible degradation reactions include disruption and rearrangement of the oxazole ring, chain scission and/or crosslinking reactions. ATR-FTIR was used to determine the nature of the chemical changes near the fiber surface. The spectra are shown in Figure 11. There are two clear changes observed with increased UV–vis exposure: at 500 h exposure a weak peak develops at 3200 cm^{-1} that is attributed to the stretching vibrations of a secondary N—H bond, and the increase in intensity with exposure of a peak at $\sim$ 1685 cm^{-1} that is assigned to the C—O of an amide linkage. Similar changes have been observed by Villar-Rodil in his work monitoring chemical changes during the early stages of thermal degradation.[19] These spectra suggest that the primary degradation pathway is disruption of the oxazole ring to form an amide linkage. Chain scission is not indicated as one likely outcome of that reaction would be nitrile end groups and no such absorbance was observed in the IR spectra.

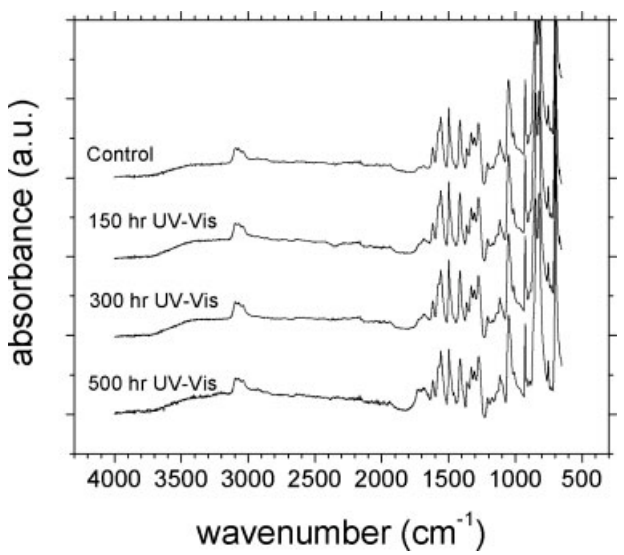

Figure 11 ATR-FTIR results for UV–vis exposed PBO AS fiber.

Table II shows the results of SAXD on UV–vis exposed fiber. The Guinier correlation length D, radius of gyration R_3, mean length of void cross section l_2, and

TABLE II
Results of Guinier Plot and SAXD Analysis for PBO AS Fiber Exposed to UV–visible Light

Sample (d)	D (Å)	R_3 (Å)	l_2 (Å)	S_3 (Å^2)
Control	34.6	31.1	42.4	12.03
150	32.7	32.4	42.5	18.83
200	32.7	32.9	43.0	17.86
270	33.7	32.1	42.3	14.80
300	31.9	32.9	43.0	17.79

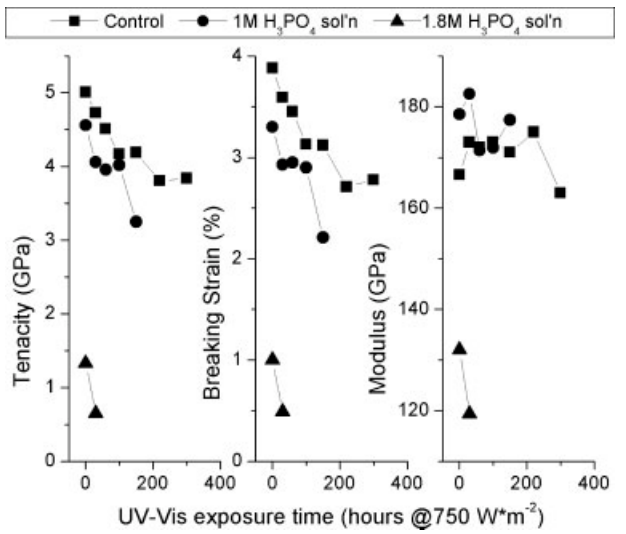

Figure 12 Mechanical properties of phosphoric acid exposed PBO AS fibers with UV–visible light.

void cross section area S_3 appear to not be significantly altered by UV–visible light exposure.

In total this data suggests that UV–vis degradation is a chemical process occurring on the fiber surface in which the cyclic structure of the PBO backbone is disrupted and an amide linkage formed. This may occur without chain scission. Even a relatively small degree of degradation on the surface of the fiber will result in a significant loss in cross-sectional area, and in addition the material lost is from the highly ordered shell region of the fiber.

UV–visible light exposure/phosphoric acid exposure

Mechanical tests were conducted on filaments after UV–vis light exposure on both phosphoric acid conditioned and control samples. Figure 12 shows how the fiber tenacity and elongation change with increased exposure time. Note in both graphs, the squares are results on fibers without any conditioning in PA/H_2O solution, the circles are results from a 1*M* solution, and the triangles represent findings from a 1.8*M* solution. These, in turn, translate into residual phosphorus of 0.3, 0.7, and 4.8 wt % respectively. It can be seen in all cases that exposure to UV–vis light causes a reduction in both the stress elongation to break. Figure 12 also shows that small amounts of additional residual PA dramatically enhance the degradation in mechanical properties. This finding supports the first hypothesis in arguing that residual PA plays a role in the degradation process and underscores the importance of thorough extraction of residual PA in any attempt to alleviate fiber degradation. It should be noted that at 4.8% residual PA, the fibers were so degraded that measurements were not possible after more than 50 h exposure. Modulus was measured and is in the range of 170 $\pm$ 5 GPa and is independent of exposure time for control fibers and fibers soaked in 1M PA/H_2O solution. The phosphoric acid soaked and UV-vis exposed fibers show a more dominant influence of fiber strength and elongation at break than on modulus. Only when the exposure time approaches 300 h there is an indication of a slight decrease. However, for fibers soaked in 1.8 M PA/H_2O solution, where the residual phosphorus concentration is 4.8 wt %, the modulus decreases after soaking as well as after exposure, which is similar to the change in strength and elongation-at-break. Compared to the modulus, the phosphoric acid soaking and UV–vis light exposure samples show a more dominant influence on the fiber strength and elongation-at-break.

CONCLUSIONS

Degradation of mechanical properties from exposure to moisture appears to be primarily due to swelling of the fiber which separates the fibrillar elements and introduces a larger number and larger average size defect. The defects act as fracture initiation sites and the strength of the fiber drops off exponentially with the increase. IR spectroscopy and wide angle X-ray experiments indicate that there is little or no chemical change occurring with exposure to water alone thereby casting some doubt on the role that residual phosphoric acid plays in chemically degrading PBO fiber.

However, the results of tensile testing, SEM and ATR-FTIR, in which PBO fibers are exposed to high concentrations of phosphoric acid show that in addition to a chemical degradation involving hydrolysis of the oxazole ring and leading to formation of cyclic amines and amide linkages, the presence of phosphoric acid seems to accelerate the separation of fibrillar elements within the fiber structure. This is relevant to the case of moisture exposure because even small amounts of acid due to residual phosphoric acid from the spinning process may be involved in the swelling observed for moisture exposure alone.

Degradation from exposure to radiation from the UV–vis spectrum shows significant loss of mechanical properties in a short period of time. The material near the fiber surface is chemically degraded and shows loss of orientation. Infrared spectroscopy indicates that the surface has undergone hydrolysis at the oxazole ring causing disruption of the ring structure and introduction of amide linkages. SAXD experiments probing defect size indicates that the axially oriented voids are changed but little by UV–vis radiation and we conclude that the degradation is confined to the fiber surface and that the drop in mechanical properties is due to the loss in cross-sectional area available to support load, particularly important is that the UV–vis degradation is concentrated in the more highly ordered shell region of the fiber and that the core material that

remains is less ordered and has a higher concentration of voids than the shell.

The effect of exposure to phosphoric acid followed by UV–vis exposure shows that the loss of both breaking strength and elongation at break increased with exposure to increasingly acidic environments. These results support the idea that even the relatively low concentrations of residual phosphoric acid may play a large role in separating the fibrillar elements of the PBO fiber.

In sum we can say that the most significant degradation mechanism for PBO AS fiber is the loosening of the fiber structure due to moisture and/or phosphoric acid. UV–vis degradation is significant also, but it should prove to be much easier to prevent this type of environmental damage than to exclude moisture in a typical service environment. Possible approaches to alleviate damage due to moisture include removing the residual phosphoric acid by washing the fibers with an inert solvent such as supercritical carbon dioxide, neutralizing the residual acid using small basic molecules and excluding moisture from the fiber surface with a barrier film that may also absorb radiation in from the UV–vis spectrum.

It is perhaps useful to also consider that because the loss of strength is primarily due to loosening of the fiber morphology there is actually an opportunity to improve the properties of PBO. Any postspinning process we can introduce that compacts the structure of the fiber, increases the size of the fibrillar elements and reduces the volume fraction of voids should be a route to improving the mechanical properties. These approaches to alleviating environmental degradation and improving the base fiber properties are presented and assessed in Part II of this paper.

References

1. Percha, P. A. Mater Res Soc Symp Proc 1989, 134, 307.
2. Kumar, S. Mater Res Soc Symp Proc 1989, 134, 360.
3. Denny, L. R. Mater Res Soc Symp Proc 1989, 134, 395.
4. Farris, R. J. Mater Res Soc Symp Proc 1989, 134, 297.
5. Toyobo. http://www.toyobo.co.jp/e/seihin/kc/pbo/technical.pdf, Toyobo Co., 2001, pp 2–18.
6. AP. In New York Times, New York, 2003, p A37.
7. Thomas, E. L. Polym Eng Sci 1985, 25, 1093.
8. Thomas, E. L. Macromolecules 1988, 21, 433.
9. Thomas, E. L. Macromolecules 1988, 21, 436.
10. Pottick, L. A. Polymer Science and Engineering, University of Massachusetts, Amherst, Ph. D. Dissertation, 1986.
11. Minter, J. R. In Polymer Science and Engineering, University of Massachusetts, Amherst, Ph. D. Dissertation, 1982.
12. Berry, G. C. ACS Polymer Preprints, 1979, 20, 42–44.
13. Metzger, P. C. Carnegie-Mellon University, Pittsburgh, 1980.
14. So, Y.-H. J Polym Sci, Part A: Polym Chem 1999, 37, 2637.
15. Bourbigot, S. Polym Int 2001, 50, 157.
16. Wang, S. Macromolecules 2004, 37, 3815.
17. Kitigawa, T. J Polym Sci, Part B: Polym Phys 1998, 36, 39.
18. Shioya, M. J Appl Phys 1985, 58, 4074.
19. Villar-Rodil, S. Chem Mater 2003, 15, 4052.